Adding Shaft Angle Measurement to Generator Protection and Monitoring

Greg Zweigle and Dale Finney, *Schweitzer Engineering Laboratories, Inc.*
Roy Moxley, *formerly of Schweitzer Engineering Laboratories, Inc.*

***Abstract*—Traditional protective relays for generators have used electrical quantities (current and voltage) to measure the condition of the machine. It has long been recognized that information about the machine can also be used in protection. New technology makes it possible to combine mechanical and electrical inputs. This paper examines the use of rotor shaft angle measurement in a generator combined with the electrical angle of the output voltage. This provides for the direct measurement of system conditions that could only be estimated or approximated with earlier technologies. Some of the protection, control, and situational awareness applications now possible include the following:**

- **Subsynchronous resonance detection and mitigation**
- **Out-of-step detection**
- **Machine parameter estimation and validation**
- **Transient stability control**

One significant improvement over previous applications that provided these functions is that no physical connection or significant modification of the shaft is necessary. As power grids operate closer to critical stability limits, the ability to measure and control precise shaft angle will provide the high reliability necessary for electric power.

I. Introduction

The addition of new measurements in power systems has always advanced protection and control systems to improve performance. Initial power distribution facilities used a measurement of current to indicate a circuit overload, in which case, an operator would interrupt the power. This was improved with relay measurement of current initiating a circuit breaker operation. The addition of voltage measurement brought about the distance relay, and added elements, such as frequency and rate of change, brought further improvements [1].

Mechanical measurements have long been a part of machine protection. Speed, vibration, shaft strain, pressure, and other physical measurements are brought into a generator control system to prevent generator damage and improve operating performance.

The innovation discussed in this paper demonstrates a time-synchronized mechanical measurement and shows how to use it to provide new power system applications.

II. Generator Shaft Measurement Technique

There are a number of ways of measuring the spinning generator shaft. Toothed wheels with magnetic pickups provide speed and acceleration measurements. Strain measurements along the shaft can measure torque and indicate stress to the shaft from system events or operating conditions [2]. While these measurements have proven useful, they also bring their own operating issues. For instance, shaft-mounted strain gauges require slip rings or wireless telemetry to transmit their measurements.

Another issue is that toothed wheel with magnetic pickup technology requires the toothed wheel to be an integral part of the shaft, with the magnetic pickup mounted in close proximity. A machine might initially be installed with a toothed wheel in place, or an existing shaft gear might be instrumented. If these options are not available, a machine retrofit may be required, which, in certain configurations, can be difficult or impossible. An advantage of this technology is that it is not impacted by dust or other contaminants. It can also provide a large number of pulses per shaft revolution. This gives high resolution to disturbances or short pulses of acceleration and deceleration.

External to the machine, terminal voltage and current measurements allow the detection of some internal conditions. For example, loss of field causes a change in apparent impedance characteristics [1] calculated by measuring voltage and current values. Out-of-step conditions, sometimes referred to as pole slipping, are indicated by measuring an impedance swing or using swing center voltage to determine a swing [3].

These measurement approaches do not provide a time-synchronized input, at least not with the level of timing accuracy that can be accomplished by integrating a shaft measurement into an overall synchrophasor system. Meanwhile, methods have been proposed for measuring time-synchronized rotor angles [4] [5], and interest in obtaining direct internal machine state measurements with accurate time stamps is increasing [6].

A prototype system was built to demonstrate time-synchronized rotor angle measurement concepts. The measurement approach was selected to facilitate simple retrofits on existing generator shafts. A laser is mounted on the generator and pointed at the shaft. Reflective tape is applied to a fraction of the circumference of the shaft. The light beam is reflected from the tape to an optical pickup. Fig. 1 shows a diagram of the setup.

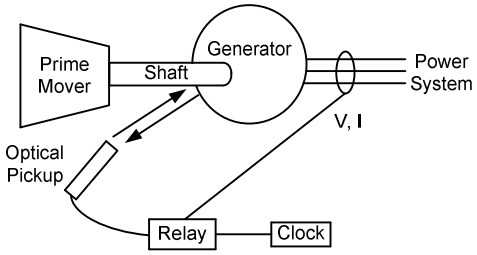

Fig. 1. Rotor angle measurement system

The data are then input to the relay, where the rising and falling edges are detected and time-stamped with microsecond accuracy. Although the generator may have significant vibration, some of the vibration is canceled if it is common to both the shaft and machine. A practical system may use several sensors to measure angle at different points on the shaft system of a large turbogenerator.

In addition, the relay can acquire synchronized measurements of the field current and voltage and the outputs of the generator automatic voltage regulator (AVR) and power system stabilizer via transducer inputs.

III. Subsynchronous Resonance

A number of local and wide-area applications enabled by time-synchronized measurements of internal machine states are possible. The first is the measurement of torsional vibration for detection of subsynchronous resonance (SSR). These resonance conditions are caused by undamped exchanges of energy between the electrical system of the power grid and the mechanical system of the generator. As such, the resonances are, to some degree, in both the mechanical and electrical systems. The frequency of SSR varies depending on machine and system parameters, but 26 Hz is a common value, and a range of 18 to 35 Hz is possible [7].

Synchronized phasor measurements of terminal signals can give an indication of these oscillations. However, the filter response of a typical phasor measurement unit (PMU) is designed to meet the requirements of IEEE C37.118 [6], which is not necessarily suitable for the lower frequencies of SSR.

In the PMU filter response in Fig. 2, the narrow response is typical of IEEE C37.118.1 requirements and the wide response is a setting option outside of those requirements but with a broader frequency band. In order to see a 26 Hz oscillation, the frequency response of the filter must have minimal attenuation well below the nominal frequency (60 Hz in this case). As shown in Fig. 2, the narrow response has virtually no signal at 26 Hz, while even the wide response has some attenuation.

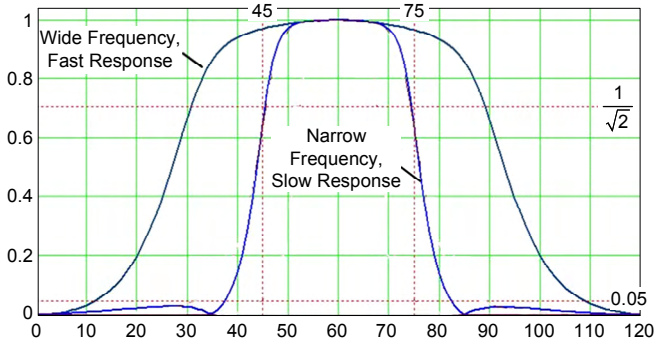

Fig. 2. PMU filter response

Shaft measurements, on the other hand, do not have the same rejection requirements as synchrophasors. In the case of SSR detection, filtering is only necessary to remove noise signals and provide anti-aliasing band-limiting. SSR itself is of concern when an undamped oscillation occurs, so a modal analysis to determine damping of oscillations in the machine resonant range is the primary calculation required.

Combining electrical and mechanical measurements in a perfectly synchronized manner improves the accuracy of SSR detection, which remains an ongoing issue [8]. By simultaneously measuring the electrical inputs of the generator and the mechanical response of the shaft, SSR is directly measured, as long as filters on the electrical signals do not reject the frequencies of interest.

The link between SSR and series-compensated transmission lines has long been recognized. More recently, it has been shown that active power system components, such as a VAR flicker controller in a nearby steel mill or a slip recovery drive on a large motor, can also induce resonance [9]. In certain situations, the resonant frequency can be supersynchronous, above the nominal power system frequency. A time-synchronized system is useful in the identification of these sources.

IV. Out-of-Step Detection

We can simplify a system to illustrate electrical out-of-step detection, as shown in Fig. 3 [3].

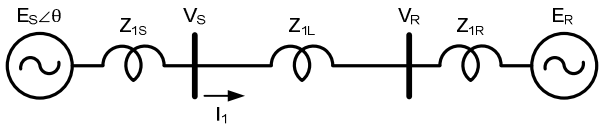

Fig. 3. Simplified two-source model for out-of-step detection

If only measurements at the buses are available, assuming E_s and Z_s are buried inside the generator and not measurable, then there are several techniques for detecting an out-of-step condition that try to limit the impact of this measurement restriction.

Traditional out-of-step detection is done by timing the trajectory of the apparent impedance between regions in the complex RX plane, as shown in Fig. 4 [3]. If the impedance crosses the inner *Z* and outer *Z* regions slowly enough, then an out-of-step condition is declared.

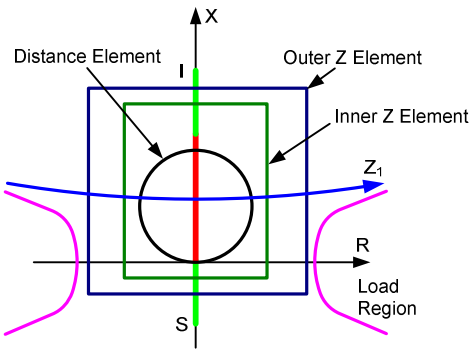

Fig. 4. Quadrilateral impedance-based power swing detection characteristic

Setting the outer *Z* and inner *Z* boundary levels correctly, along with defining the threshold below which a crossing is sufficiently slow, requires considerable knowledge of the system in order to determine the maximum speed of the impedance swing between these boundaries. This may or may not be possible, depending not only on the knowledge of the system state but also on how that state may change over time. For instance, during a major system disturbance, the impedance locus may jump instantaneously due to the loss of a generator or transmission line elsewhere in the power system.

An improvement on this method using the concept of swing center voltage (SCV) was introduced in [3] and is shown in Fig. 5.

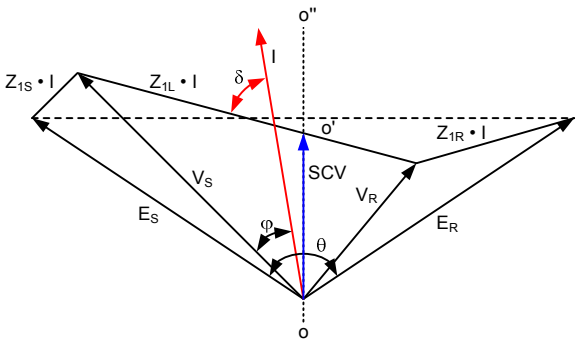

Fig. 5. Voltage phasor diagram of two-source system

Because direct measurements of E_S and E_R are typically unavailable, they must be approximated. Using internal machine measurements, these values can be used directly with improved accuracy and performance.

A centralized out-of-step detection scheme can be implemented using synchrophasor technology. An example system is shown in Fig. 6.

Synchronized measurements of bus voltages are collected throughout the system. The angle differences between each bus can then be determined. Angle difference is further processed to calculate acceleration and slip frequency in order to detect an out-of-step condition [10]. Using shaft angle measurements, this scheme can be extended to detect swings that pass through a generator or generator step-up transformer (see Swing 2 in Fig. 6). As a result, out-of-step detection becomes more precise, and improved control of the system, with better selection of appropriate system separation points, then follows.

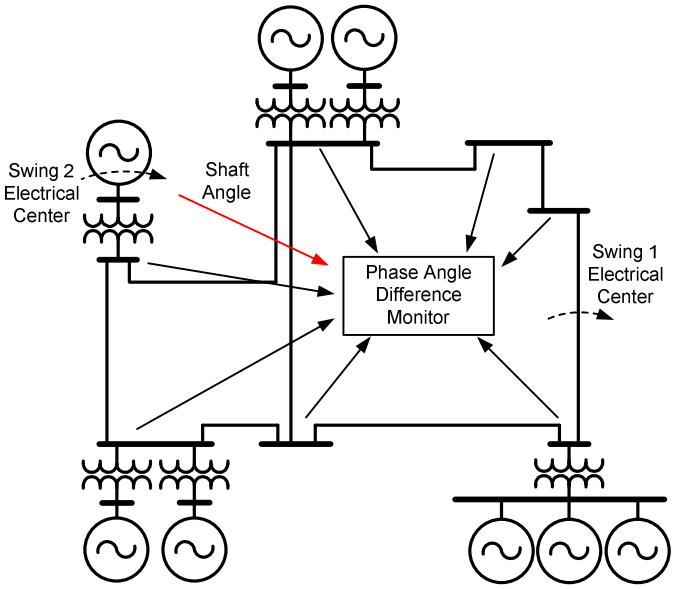

Fig. 6. Centralized out-of-step detection scheme

V. Parameter Measurement and Estimation

Prior to the adoption of time-synchronized phasors, the measurable electric power network quantities were voltage magnitude, current magnitude, and power transfer. Based on these measurements, the unknown quantities, such as the voltage angle and current angle, were estimated with a nonlinear approach. Now, with the addition of network angle measurements, nonlinear estimation is no longer required and the network state is directly measurable. Additionally, with rotor angle measurements, even machine states are moving into the domain of direct, time-synchronized measurement technology.

It might seem that direct network state measurement obsoletes nonlinear estimation in power system analysis. However, in addition to the network state, it is helpful to know other features of the electric power system, such as the parameters of connected devices. Many of these parameters require dedicated test setups and are estimated offline. This not only makes the estimation of some parameters expensive but also means they are not known in real time. With the addition of time-synchronized rotor angle measurements, it becomes possible to estimate certain machine parameters using off-the-shelf PMU technology. This simplifies parameter estimation and makes it possible to measure parameters continuously during normal machine operation.

Machine parameter estimation is a large area of study [11] [12]. One possible method of estimating these parameters, which is based on time-synchronized measurements, is outlined here. This example is meant to illustrate the concept,

not to comprehensively cover the subject area. As demonstrated in Section IV, the out-of-step condition is a function of the internal voltage (denoted as E' instead of E_s in this section) and transient reactance (denoted as X'_d instead of Z_s in this section). These values are part of what is known as the classical machine model and are used in the equal area criteria [13]. The steady-state relationship for this model [14], ignoring stator resistance, is given in (1).

$$jX'_d I e^{j\phi} = E' e^{j\theta} - V e^{j\delta} \tag{1}$$

The objective is to solve for E' and X'_d based on the measured terminal current $Ie^{j\phi}$, the measured terminal voltage $Ve^{j\delta}$, and the rotor angle θ. The first step is converting (1) to rectangular coordinates.

$$I\cos(\phi) + jI\sin(\phi) = \frac{1}{jX'_d}(E'\cos(\theta) - V\cos(\delta)) + \frac{j}{jX'_d}(E'\sin(\theta) - V\sin(\delta)) \tag{2}$$

Next, equate the real and imaginary parts of (2).

$$\begin{aligned} X'_d I\cos(\phi) &= E'\sin(\theta) - V\sin(\delta) \\ X'_d I\sin(\phi) &= V\cos(\delta) - E'\cos(\theta) \end{aligned} \tag{3}$$

Now, because the measurements are time-synchronized, it is possible to reference all angles to the rotor angle θ.

$$\begin{aligned} X'_d I\cos(\phi - \theta) &= -V\sin(\delta - \theta) \\ X'_d I\sin(\phi - \theta) &= V\cos(\delta - \theta) - E' \end{aligned} \tag{4}$$

The result shown in (4) separates E' and X'_d from the nonlinear sinusoidal terms. Therefore, straight substitutions isolate these terms and give the final estimate.

$$\begin{aligned} X'_d &= -\frac{V \bullet \sin(\delta - \theta)}{I \bullet \cos(\varphi - \theta)} \\ E' &= V\cos(\delta - \theta) + V\sin(\delta - \theta)\tan(\phi - \theta) \end{aligned} \tag{5}$$

A system to estimate E' and X'_d is physically connected as shown in Fig. 1. At each time step, the PMU measurements of terminal voltage (both magnitude and angle), current (magnitude and angle), and rotor angle are substituted into (5). The results are then filtered with a low-pass filter to reject noise and improve the estimate accuracy.

An important consideration is the effect of measurement error on the accuracy of the estimates. IEEE C37.118.1 specifies measurement error according to a definition called the total vector error (TVE). The standard requires better than 1 percent TVE for synchrophasor measurements. This requirement applies over the full measured frequency range of ±5 Hz around nominal frequency. Typically, a PMU is much more accurate than 1 percent in the normal operating frequency range. For example, in the range of ±100 mHz around nominal frequency, a typical PMU is better than 0.25 percent TVE. When estimating machine parameters, a frequency condition check is placed prior to the estimate.

A set of simulations was run to determine the accuracy of the estimated parameters as a function of the measurement errors. The terminal voltage and current errors were held constant at 0.25 percent TVE. Then the angle portion of these measurements was rotated, as shown in Fig. 7, while the overall 0.25 percent TVE was kept. All measurements within the circle shown in Fig. 7 are 0.25 percent TVE accurate.

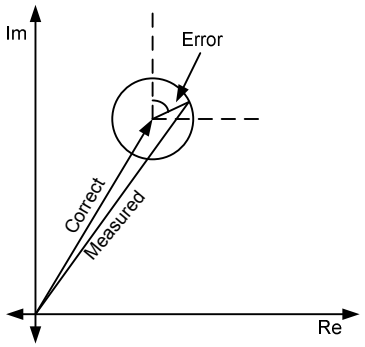

Fig. 7. Measurement error definition

The requirement for maximum rotor angle measurement error is not specified by a standard, such as IEEE C37.118.1. For the experiments in this section, rotor angle errors of 0 degrees, ±0.25 degrees, and ±0.5 degrees were selected. The results are shown in Fig. 8 for estimates of E' and Fig. 9 for estimates of X'_d. In Fig. 8 and Fig. 9, the vertical axis is the percent error in the estimate and the horizontal axis is the rotation of the electrical signal vector at the PMU. Some of this variation with angle error is smoothed by post-estimation filtering, and the resulting estimation error is an average of the graphed value. There are three curves in each graph, one for each value of rotor angle measurement error. The lower, solid curve is for an exact rotor angle measurement. The middle, dotted curve is for 0.25 degrees of rotor angle measurement error. The upper, dashed curve is for 0.5 degrees of error.

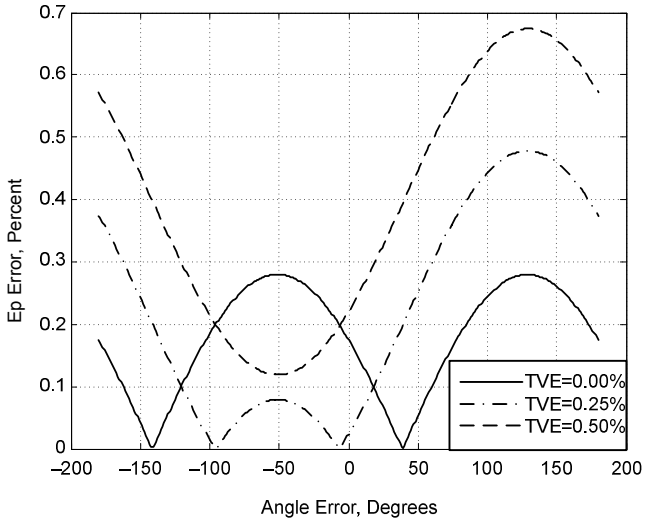

Fig. 8. The error in estimated E' as a percent of the correct value

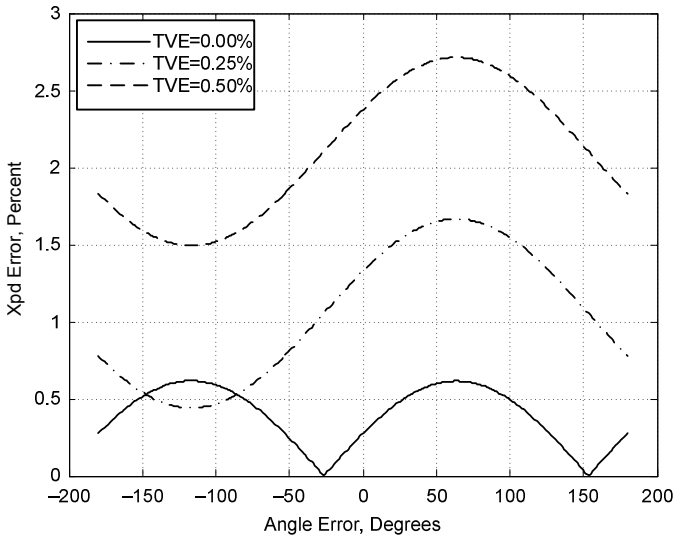

Fig. 9. The error in X'_d as a percent of the correct value

VI. Transient Stability Control

The final application of rotor angle measurements is the use of a time-synchronized measured state, with both network variables and machine variables, as part of a wide-area, transient, stability-oriented control scheme. Direct measurements bypass the need for intermediate state variable estimates, which helps improve the response speed that is important for transient stability applications. Furthermore, with the addition of machine states in these measurements, a very accurate initial state enables a new method for mitigating transient instability.

Present remedial action schemes rely in part on offline system simulations during the planning phase. These simulations are based on expected contingencies, and the resulting systems are reliable. However, as the number of expected contingencies increases, it becomes very difficult to anticipate and design a response for each. Another challenge for remedial action scheme design is uncertainty in models and model parameters. Compensation for modeling inaccuracy results in responses that are sometimes more conservative than necessary.

By leveraging the time-synchronized network and machine states, a feedback control method to resolve transient instabilities was designed [15]. The system iterates the control selection at specific intervals, and each iteration initializes with a new time-synchronized measured state. Control actions are then selected by anticipating the future response of the system and comparing the response for a set of controls against a performance measure. The best control is selected from the set and applied to the system at each iteration.

Fig. 10 shows the approach, which is related to model predictive control techniques [16]. The system experiences a disturbance, such as a line fault, at time t_F. Until time t_T in Fig. 10, the system is evolving according to its dynamics. At time t_T, the control scheme begins the process of selecting an appropriate control. A set of predictions is shown in Fig. 10, starting at t_T. In this example, the following three possible sequences of control actions are considered:

- Predicted trajectory for no controls, where no control actions are initiated by the controller.
- Predicted Trajectory 1, where Control Sequence 1 is applied to the system.
- Predicted Trajectory 2, where Control Sequence 2 is applied to the system.

The reference trajectory, which represents the desired trajectory, is also shown. The wide-area control algorithm selects the control sequence that results in a trajectory with minimal cost compared to the reference trajectory. After applying the control sequence, the system is allowed to evolve for a previously specified duration of time, and then the entire algorithm repeats. Each repetition starts with a complete time-synchronized measured state. The process of iterating the algorithm and starting the iterations with new measurements results in a set of controls with improved robustness to both modeling and measuring errors.

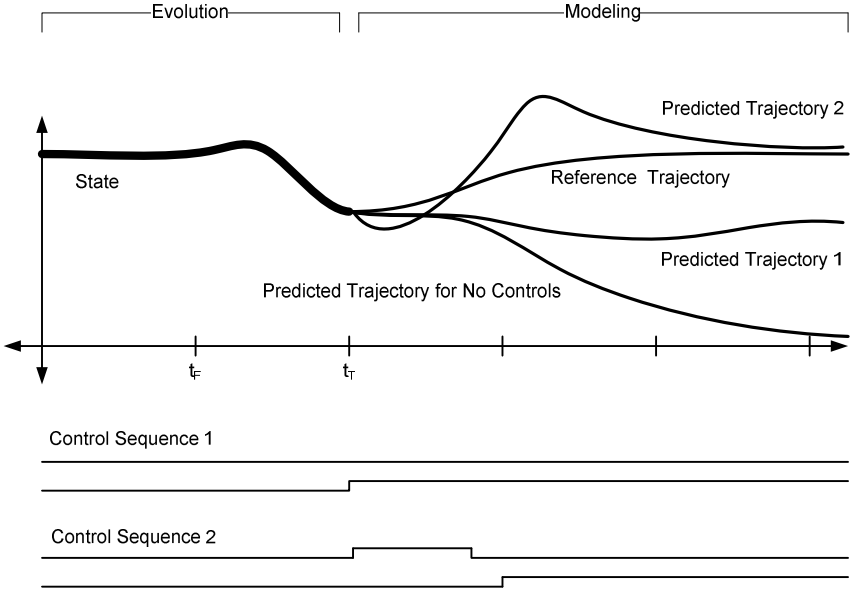

Fig. 10. Prediction approach

The general form of the system model is given by (6). Machine state variables are $\underline{x}$, and the network state variables are $\underline{y}$. The function f($\underline{x}$, $\underline{y}$) is the set of machine differential equations. A two-axis model is used [13], and the model also includes an AVR and governor. The function g($\underline{x}$, $\underline{y}$) is the set of power flow equations for the network.

$$\begin{aligned} \dot{\underline{x}} &= f(\underline{x}, \underline{y}) \\ \underline{0} &= g(\underline{x}, \underline{y}) \end{aligned} \tag{6}$$

A performance metric is selected to minimize the square of the difference between the predicted system states and the desired states. This difference is multiplied by the cost of the controls. Equation (7) provides the cost function for a single state, and multiple states extend (7) by including sums over the additional states. The variable q_i is a state variable, and *i* is a time-based index. The variable $q_i^{(o)}$ is the desired value of the state variable. The state variable cost is over K' integration steps. These are the integration intervals over which (6) is computed, starting with a set of directly measured time-synchronized states. The function $C(u_{k+1},\ldots,u_{k+K})$ is the cost of the controls and is over *K* prediction steps. A set of controls, *u*, is selected that minimizes (7).

$$\min_{u}\left\{\left(\sum_{i=k+1}^{k+K'} Q\left(q_i - q_i^{(o)}\right)^2\right) C\left(u_{k+1},\ldots,u_{k+K}\right)\right\} \tag{7}$$

The cost of the controls is given by Table I. In this example, there are two possible controls. One is shedding generation, and the other is insertion of a series line capacitor. Other control options, such as load shedding and insertion of a dynamic brake, are also possible for transient stability applications. The numerical values of the control options are selected as integers to keep the example simple. Various different numerical values are possible and, in most cases, are specific to the application.

TABLE I
CONTROL COSTS

No-Control Result	No Action	Series Capacitance	Generation Shedding
Stable	1	2	∞
Unstable	2	1	3

As an experimental test, the wide-area control algorithm was applied to a large contingency on the IEEE 39-bus system. A diagram of this system is shown in Fig. 11, along with the location of three simultaneous faults. Although such a severe fault is unlikely, it is selected as a worst-case scenario to demonstrate the capabilities of a control scheme that makes control decisions based on real-time state measurements.

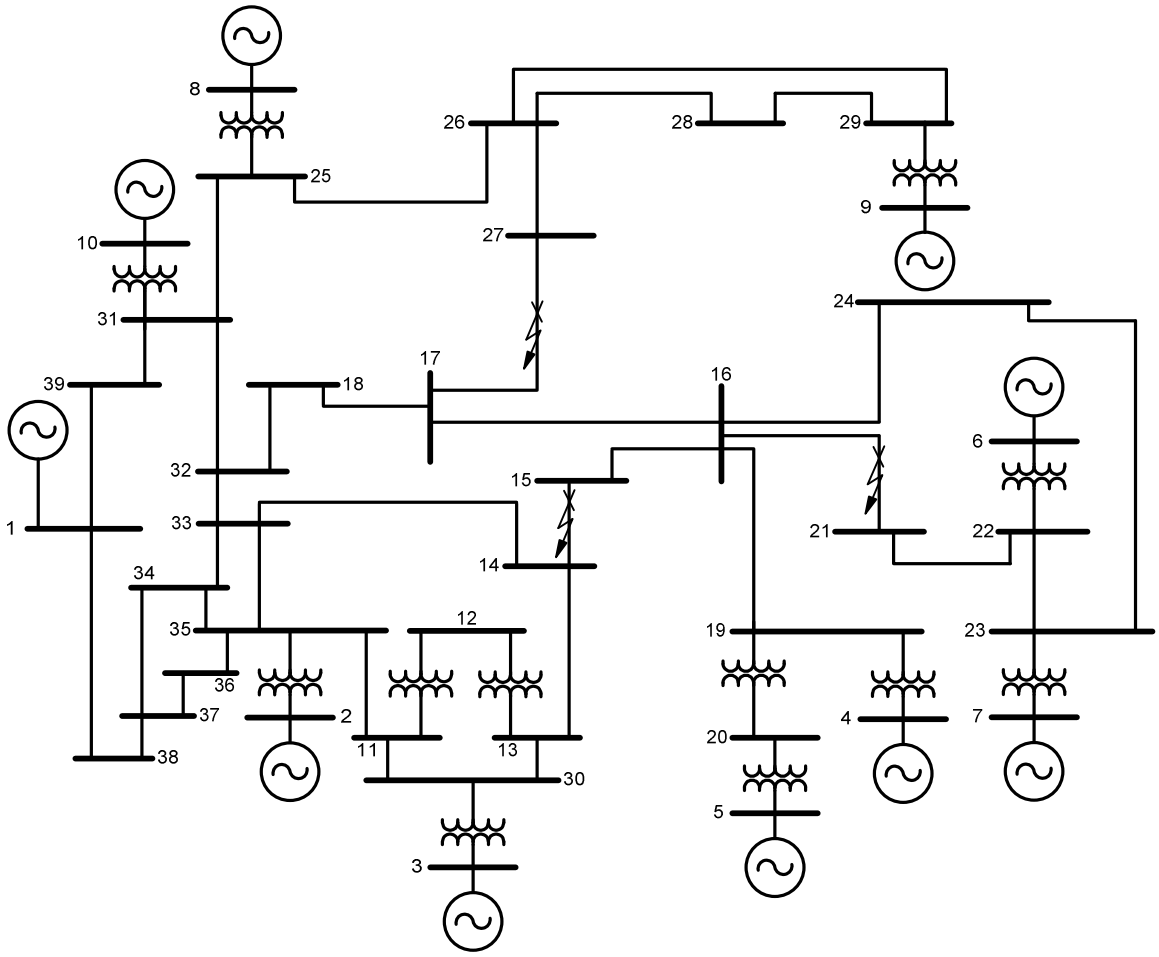

Fig. 11. Example system

The response of the generator rotor angles to these faults is given in Fig. 12. Generators 6 and 7 (designated by their bus numbers) accelerate away from the rest of the system, indicating instability.

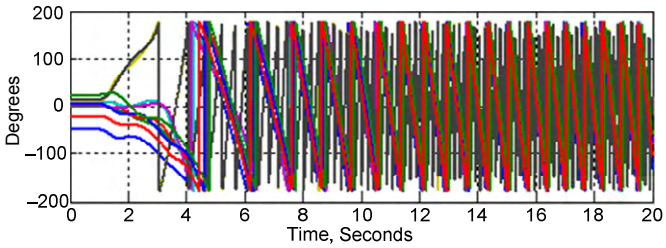

Fig. 12. Response of the system without control application

For this example, the wide-area control algorithm runs every 50 milliseconds. This allows for communications and processing delays. The prediction window (determined by K') is set at 2 seconds, and the number of sequential controls considered (determined by *K*) is set at two controls, per (7). Considering more controls improves the performance of the system because a more optimal set of controls is realized. However, the disadvantage is an increase in computational time. A wide margin for the parameter errors is tested by including a random 10 percent uncertainty applied to all parameters for the prediction model.

When the control algorithm is applied to the example of Fig. 12, it selects tripping Generator 7 as the means to stabilize the system. After Generator 7 is disconnected, the remaining system comes back into synchronization without the need for any further controls. This includes not requiring the shedding of Generator 6, which had also lost synchronization with the rest of the system prior to the control application. An advantage of the proposed algorithm is that states are measured with precise time stamps in real time and used directly to select control actions, which can result in lower impact control selection. The history of state measurements, along with the history of previous control actions, allows a least-cost solution to stabilize the system. Instead of removing Generator 6 and 7, only Generator 7 is tripped. Fig. 13 shows the response of the system rotor angles with this control scheme.

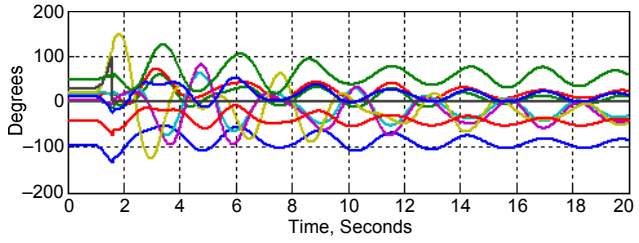

Fig. 13. Response of the system with predictive control application

VII. Conclusion

As with prior additions to measurement systems, synchronized measurement of shaft position provides new capabilities as well as new challenges. Integrating synchronized shaft measurements into complete protection and control schemes improves the security of protection schemes and provides new control capabilities. The monitoring of subsynchronous resonances is improved by having a measurement at the rotor shaft. Estimation of internal machine parameters is improved with direct measurement of machine states. Finally, synchronized machine and network measurements can allow new methods of predictive control that exhibit reduced susceptibility to parameter errors.

VIII. References

[1] C. R. Mason, *The Art and Science of Protective Relaying*. John Wiley & Sons, Inc., New York, 1956.

[2] M. Newby and R. Scheepers, "Quantification and Management of Grid Interaction Effects on Turbo-Generator Sets," proceedings of the 18th World Conference on Nondestructive Testing, Durban, South Africa, April 2012.

[3] N. Fischer, G. Benmouyal, D. Hou, D. Tziouvaras, J. Byrne-Finley, and B. Smyth, "Do System Impedances Really Affect Power Swings – Applying Power Swing Protection Elements Without Complex System Studies," proceedings of the 65th Annual Conference for Protective Relay Engineers, College Station, TX, April 2012.

[4] Y. Chen, C. Zhang, Z. Hu, and X. Wang, "A New Approach to Real Time Measurement of Power Angles of Generators at Different Locations for Stability Control," proceedings of the IEEE Power Engineering Society Winter Meeting, Singapore, January 2000.

[5] Q. Yang, T. Bi, and J. Wu, "WAMS Implementation in China and the Challenges for Bulk Power System Protection," proceedings of the IEEE Power Engineering Society General Meeting, Tampa, FL, June 2007.

[6] IEEE C37.118.1-2011, IEEE Standard for Synchrophasor Measurements for Power Systems.

[7] K. Kabiri, H. W. Dommel, and S. Henschel, "A Simplified System for Subsynchronous Resonance Studies," proceedings of the International Conference on Power Systems Transients, Rio de Janeiro, Brazil, June 2001.

[8] M. Elfayoumy and C. Grande Moran, "A Comprehensive Approach for Sub-Synchronous Resonance Screening Analysis Using Frequency Scanning Technique," proceedings of the IEEE Power Tech Conference, Bologna, Italy, June 2003.

[9] L. S. Dorfman and M. Trubelja, "Torsional Monitoring of Turbine-Generators for Incipient Failure Detection," proceedings of the 6th EPRI Turbine Generator Technology Transfer Workshop and Turbine Generator Users Group Meeting, St. Louis, MO, August 1999.

[10] E. O. Schweitzer, III, D. Whitehead, A. Guzmán, Y. Gong, and M. Donolo, "Advanced Real-Time Synchrophasor Applications," proceedings of the 35th Annual Western Protective Relay Conference, Spokane, WA, October 2008.

[11] Power Systems Engineering Research Center, "Estimation of Synchronous Generator Parameters From On-Line Measurements," PSERC Publication 05-36, June 2005. Available: http://www.pserc.wisc.edu/documents/publications/reports/2005_reports/heydt_synchronousgenerator_finalreport_s15_7june2005.pdf

[12] C. T. Huang, Y. T. Chen, C. L. Chang, C. Y. Huang, H. D. Chiang, and J. C. Wang, "On-Line Measurement-Based Model Parameter Estimation for Synchronous Generators: Model Development and Identification Schemes," *IEEE Transactions on Energy Conversion*, Vol. 9, Issue 2, June 1994.

[13] P. Kundur, *Power System Stability and Control*. McGraw-Hill, Inc., New York, 1994.

[14] N. Fischer, G. Benmouyal, and S. Samineni, "Tutorial on the Impact of the Synchronous Generator Model on Protection Studies," proceedings of the 35th Annual Western Protective Relaying Conference, Spokane, WA, October 2008.

[15] G. Zweigle and V. Venkatasubramanian, "Model Prediction Based Transient Stability Control," proceedings of the IEEE PES Transmission and Distribution Conference and Exposition, Orlando, FL, May 2012.

[16] J. B. Rawlings, "Tutorial Overview of Model Predictive Control," *IEEE Control Systems Magazine*, June 2000, pp. 38–52.

IX. Biographies

Greg Zweigle received his M.S. in electrical engineering and M.S. in chemistry from Washington State University. He also received a B.S. in physics from Northwest Nazarene University. He is presently a principal research engineer at Schweitzer Engineering Laboratories, Inc. Greg holds seven patents and is pursuing a Ph.D. in energy systems. He is a member of IEEE and the American Chemical Society.

Dale Finney received his bachelor of engineering degree from Lakehead University and his master of engineering degree from the University of Toronto. He began his career with Ontario Hydro, where he worked as a protection and control engineer. Currently, Dale is employed as a senior power engineer with Schweitzer Engineering Laboratories, Inc. His areas of interest include generator protection, line protection, and substation automation. Dale holds a number of patents and has authored more than twenty papers in the area of power system protection. He is a member of the main committee of the IEEE PSRC, a member of the rotating machinery subcommittee, and a registered professional engineer in the province of Ontario.

Roy Moxley received his B.S. in electrical engineering from the University of Colorado. He worked for Schweitzer Engineering Laboratories, Inc. (SEL) from 2000 to 2012 as a marketing manager. He has authored and presented numerous papers at protective relay and utility conferences. Prior to joining SEL, he was with General Electric Company as a relay application engineer, transmission and distribution (T&D) field application engineer, and T&D account manager. He is a registered professional engineer in the state of Pennsylvania and a member of IEEE and CIGRE.